

# Application-Oriented Extensions of Profile Flags

Matej Mlejnek<sup>†</sup>, Pierre Ermes<sup>‡</sup>, Anna Vilanova<sup>§</sup>, Rob van der Rijt<sup>¶</sup>, Harrie van den Bosch<sup>¶</sup>, Frans Gerritsen<sup>‡</sup>, M. Eduard Gröller<sup>†</sup>

<sup>†</sup>Institute of Computer Graphics and Algorithms, Vienna University of Technology, Austria

<sup>‡</sup>Philips Medical Systems, Best, Netherlands

<sup>§</sup>Department of Biomedical Engineering, Technische Universiteit Eindhoven, Netherlands

<sup>¶</sup>Catharina Hospital, Eindhoven, Netherlands

---

## Abstract

*This paper discusses two applications of probing dense volumetric data for MR orthopedics and dynamic contrast enhanced MRI mammography. In order not to reduce the context information and to extract the essential part of the data, we apply Profile Flags. A Profile Flag is a 3D glyph for probing and annotating the volumetric data. The first application area deals with visualization of T<sub>2</sub> profiles for interactive inspection of knee cartilage and detection of lesions. In the second application, we present the usability of the Profile Flags for measuring of time-signal profiles for a set of time-dependent MR volumes. Several extensions of the basic Profile Flag concept are described in detail and discussed. These extensions include selection of a set of profiles based on spatial as well as curve differences, automatic positioning of the Profile Flags, and adaptation for probing of time-varying volumetric data. Additionally, we include the evaluation of the used methods by our medical partners.*

Categories and Subject Descriptors (according to ACM CCS): I.3.8 [Computing Methodologies-]: Computer Graphics-Applications; J.3 [Computer Applications-]: Life and medical sciences-Medical information systems

**Keywords:** visualization in medicine, applications of visualization

---

## 1. Introduction and Medical Background

In medical environments, many tools for visualization of volumetric data have been presented. These include volume rendering, multi-planar reformation, cutting planes, virtual endoscopy, etc. Most of the techniques try to classify the underlying data and enhance the essential information to be visualized. In this paper, we present several extensions and an evaluation of Profile Flags [MEV\*05], a tool for probing of profile curves in volumetric data. We apply the extensions in two application scenarios where profiles play a crucial role: MR orthopedics and MRI mammography. While the orthopedic data contains profiles, which are arranged perpendicu-

lar to a surface, the mammographic data includes time-signal profiles with specific properties.

### 1.1. MRI of articular cartilage

Articular cartilage is a thin tissue, which covers the surfaces of knee joints. Due to post-traumatic or degenerative damage, softening of the cartilage can be observed. In the next stage of the degeneration even ulceration and thinning of the cartilage may happen. This process is accompanied by pain and progressive loss of function of the tissue. An early detection of the degenerative process is essential for a successful treatment [RGWW05]. Two factors in the quantitative and qualitative characterization of cartilage degeneration are the thickness of the layer and the tissue quality, respectively. Since the cartilage is only few millimeters thick, even a subtle change in thickness and quality can indicate the progress of the disease. The classification of changes in these two im-

---

<sup>†</sup> {mlejnek|groeller}@cg.tuwien.ac.at

<sup>‡</sup> {pierre.ermes|frans.gerritsen}@philips.com

<sup>§</sup> A.Vilanova@tue.nl

<sup>¶</sup> rob@vanderrijt.nl|harrie.vd.bosch@catharina-ziekenhuis.nl

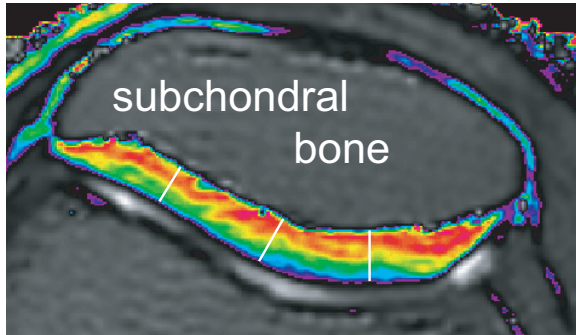


**Figure 1:** Color-coded  $T_2$  map of the articular cartilage with three locations of  $T_2$  profiles (white lines).

portant factors is essential for diagnosis and for estimating the progress of the degeneration process.

For screening of the knee cartilage, two magnetic resonance imaging (MRI) sequences are used: a high-resolution anatomical scan for the examination of the thickness and a  $T_2$  map for the evaluation of the tissue quality. In the latter the damage is represented by a disruption in the pattern of typical  $T_2$  values. In a clinical environment these two scans are usually studied on two linked screens in a slice-by-slice manner. This is a time-consuming process with reduced spatial perception, which may lead to false diagnosis. Furthermore, the communication between the radiologist and the orthopedist performing the surgery is not a trivial task, since they operate with different types of data. While the radiologist is performing the diagnosis on a stack of 2D slices, the orthopedist would need to access the volumetric information during the surgical procedures.

The disruptions of typical patterns in the  $T_2$  map can be validated by so called  $T_2$  profiles [SMD\*01, vdRvdBK\*03]. A  $T_2$  profile is a curve of varying  $T_2$  values along a line that is perpendicular to the subchondral bone and ends at the surface of the cartilage (see figure 1). Due to the arrangement of  $T_2$  values in layers parallel to the underlying subchondral bone, the  $T_2$  profiles have a typical shape for healthy cartilage.  $T_2$  profiles in areas with damaged cartilage significantly differ from these shapes. For comparison of different regions within the cartilage, multiple  $T_2$  profiles are computed and compared. A normalized  $T_2$  profile is computed in order to enable the comparison of two  $T_2$  profiles with different lengths. A normalized  $T_2$  profile is a curve which returns  $T_2$  values for the normalized distance in the interval between the subchondral bone (distance 0.0) and the articular surface (distance 1.0).

## 1.2. Breast DCE-MRI Mammography

In dynamic contrast enhanced magnetic resonance imaging (DCE-MRI) mammography, the diagnosis of a tumor is usually based on the development of time-signal profiles. These

are based on the flow of the contrast agent within the tissue. Before the acquisition of data, a contrast agent is introduced into the patient's body. This results in the increase of signal in the scanned tissue and simplifies the diagnosis of the disease. Several scans are acquired over a period of time. This process results in a set of volumes, one for each time-step. The classification of the behavior of the tissue can be determined by subtracting the pre-contrast volume from all post-contrast images. Since the acquired volumes are registered, one can generate time-signal profiles for each spatial location in the volume. Time-step 0 corresponds to the pre-contrast volume, while the following acquisition times correspond to the post-contrast volumes. The diagnosis from such time-varying data is based on the fact, that the breast tumor cells absorb and release the contrast agent in a different way than healthy breast cells. In cancerous breast regions newly formed blood vessels cause a faster inflow as well as outflow of contrast agent. Healthy regions are characterized by a low signal increase in the early post-contrast phase. Additionally three other types of time-signal profiles exist (see figure 2). Persist profiles (type 1) contain an increase of signal in the immediate and late post-contrast phase. Plateau profiles (type 2) show no change in the intensity in the intermediate and late post-contrast phases. The washout profiles (type 3) contain a significant signal decrease in the intermediate and late post-contrast phases. According to the classification, cells with persist behavior indicate benign lesions, while the plateau and washout profiles are with high probability malignant lesions [KMK\*99].

In the clinical routine, the radiologist studies a set of time-series in a slice-by-slice manner. During the first step of the investigation, he defines one or multiple suspicious regions. The diagnosis continues with the detailed inspection of the previously selected regions by computing and studying the time-signal profiles within these regions. This is a time-consuming process, which involves a high level of concentration. The suspicious regions can be very small in comparison to the spatial extent of the entire data.

The paper is structured as follows. Related work on data interaction and annotation is reviewed in section 2. The various extensions of the Profile Flags are described in detail in sections 3. In section 4, we discuss two application scenarios. Finally, we summarize and conclude the work in section 5.

## 2. Related work

Default interaction and inspection tools in a medical workstation include cutting planes, multi-planar reformation and endoscopic navigation. Recently further new interaction tools have been presented. McGuffin et al. [MTB03] presented an interactive tool for investigation of volumetric data based on different kinds of deformations and layerings of the objects. A tool for manipulation of molecular data has been presented by Huitema and van Liere [HvL00]. It com-

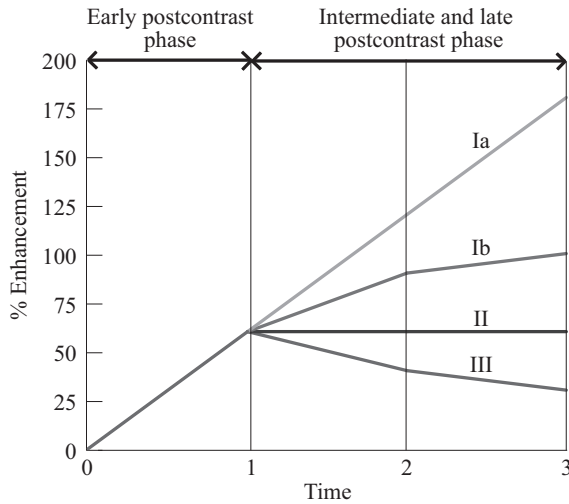


Figure 2: Four types of time-signal profiles for DCE-MRI mammography (courtesy of Coto et al. [CGB\*05]).

prises various interaction capabilities including translation or measurement instruments. For medical purposes, a framework for the measurement of angles and distances has been presented by Preim et al. [PTSP02]. Recently, annotation of volumetric structures has been widely discussed in the literature. For pre-segmented data, a feature can be annotated by a caption, which is either blended over the data [GAHS05], or located outside in a rectangular area [BG05]. De Leeuw and van Wijk [dLvW93] presented a glyph for the visualization of multi-dimensional flow data. Multiple local characteristics of flow attributes can be visualized at an arbitrary position within the data.

In our previous work, we presented the basic concept of Profile Flags [MEV\*05]. It is a glyph for the interactive probing of profiles. By dragging the glyph along the surface of the probed object, one can browse data values along lines in the tissue beneath. The profile at the position of the Profile Flag is visualized. Subramanian et al. [SBC04] presented a tool for classification of time-signal profiles for DCE-MRI data. The user specifies a time-signal profile with shape characteristics he is interested in. The system classifies the entire space of time-signal profiles according to the similarity to the pre-defined profile. Unfortunately, this approach restricts the inspection of the data to profiles similar to the pre-defined shape. Another approach by Carotenuto et al. [CEP\*04] computes False Color Maps from time-signal profiles. By classifying profiles into not overlapping regions, different areas of the volume are shown in different colors, respectively. The results of the semi-automatic detection of the suspicious profiles are visualized by maximum intensity projection. Suspicious areas are additionally color coded. Kohle et al. [KPWP02] discussed color schemes for two clinical applications: inspection of acute stroke in hu-

man brain and detection of tumors in 4D DCE images. In order not to blend the classified color-coded data, different rendering techniques, e.g., stereoscopic view, (local) maximum intensity projection, have been demonstrated. Recently, Coto et al. [CGB\*05] presented a tool analyzing breast DCE-MRI volumes. The user is provided with a set of scatterplots for all pairs of consecutive time-steps. With interactive linking and brushing in the domain of the time-signal profiles, the volume can be categorized according to the properties of the profiles. The resulting classified data are visualized with importance-driven volume rendering [VKG05].

### 3. Extensions of Profile Flags

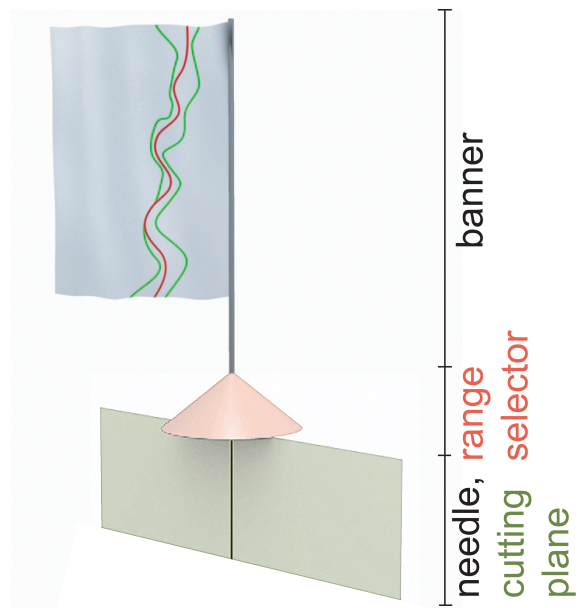
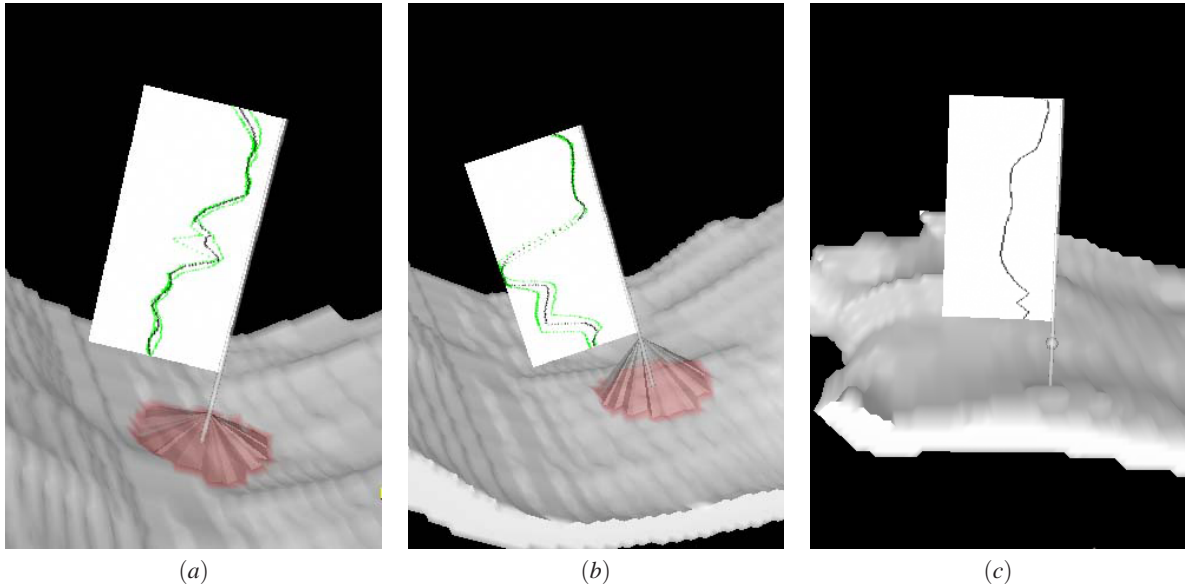


Figure 3: Profile Flag: a tool for probing of profiles [MEV\*05].

The Profile Flag [MEV\*05] is a board-pin-like glyph for probing and annotating of underlying profile data. It consists of four components: the banner, the range selector, the needle and the cutting plane (see figure 3). We discussed the use of Profile Flags for measuring  $T_2$  profiles. These are curves of varying values that are measured perpendicular to the surface of articular cartilage. The Profile Flag can be inserted on the surface of the inspected object and aligned with the normal vector of the surface in that position. For that purpose, the needle is positioned beneath the surface of the probed object. It defines the location of the reference  $T_2$  profile. Two types of needle can be selected: the fixed needle, which probes the data values along the distance from the subchondral bone, and a needle with adaptable length for measurement of normalized profiles.

The inspected profile is visualized on the banner. The top



**Figure 4:** Different approaches to visualize the thickness of the underlying tissue: (a) thin cartilage = low range selector; (b) thick cartilage = high range selector and (c) spherical marker on the flagpole.

of the banner corresponds to the upper surface of the inspected object and the bottom of the banner corresponds to the bottom surface of the object. The measured values are depicted on the horizontal axis of the banner. The right side of the banner corresponds to the lowest (0.0) measured value, while the left side of the banner corresponds to the highest value. The cone-shaped range selector is located above the surface of the object. By increasing the range selector, additional profiles in the neighborhood of the reference profile can be visualized.

According to the settings of the range selector, several types of banners can be defined. A single-profile banner shows only the reference profile at the position of the needle. By setting the radius of the range selector to a value larger than 0, either a single averaged profile is shown, or the minimal and the maximal values from all profiles in the neighborhood of the reference profile are visualized. The deviation-profile banner illustrates the difference of profiles from a reference profile defined by another Profile Flag. Thus, the deviations from the reference profile are easily perceived. The cutting-plane component of the Profile Flag is an extension of multi-planar reformation, a tool which is usually applied for inspection of  $T_2$  maps. Either the cutting plane can be rotated around the needle or the cutting plane is facing the camera and the inspected object is rotated around the needle. During investigation, one or more Profile Flags can be stuck into the inspected object. They are moved along the object's surface, while showing the underlying  $T_2$  profiles. Multiple Profile Flags can be placed to emphasize differences between profiles at different spatial locations.

In this section, we describe several extensions of the Profile Flags according to the application and, thus, the type of measured underlying data. In section 3.1, we discuss possibilities for enhancement of the glyph by incorporating the thickness information into the basic concept. In section 3.2, we show additional modi for selection of the inspected profiles. Automatic positioning of the Profile Flags is presented in section 3.3. In section 3.4 we show the extension of the Profile Flags for probing of time-varying volume data.

### 3.1. Thickness Visualization

When probing profile data, we are also interested in the thickness of the cartilage in addition to the profile itself. This can be achieved by measuring the absolute profiles, i.e., measuring the sampled values against the distance from the surface. However, this does not allow comparison of two profiles with different lengths. Another possibility is to show a normalized profile and visualize the thickness in a different way. Extending the basic metaphor of the Profile Flag allows showing the thickness information in two ways. The first approach deals with changing the height of the range selector cone. As shown in figure 4 (a),(b) the thickness of the underlying object corresponds to the height of the range selector. In order to represent the thickness and not to occlude the information rendered on the banner, the height of the range selector should be in the range between the surface of the probed object and the bottom of the banner. Knowing the range of the measured thickness values ( $t_{min}, t_{max}$ ), the entire length of the flag pole can be exploited for the visualization of the thickness. The length of the flag pole corresponds to

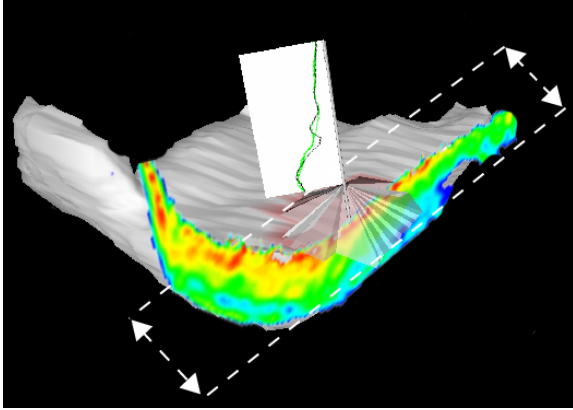


**Figure 5:** The cutting plane can be moved along its normal within the range of selected locations.

the distance between both ends of the flagpole, i.e., the surface of the object ( $h_{min}$ ) and the bottom of the banner ( $h_{max}$ ).

Then the height  $H$  of the range selector is:

$$H = h_{min} + \frac{(T - t_{min})(h_{max} - h_{min})}{(t_{max} - t_{min})}, \quad (1)$$

where  $h_{max}$  is smaller or equal to the length of the flagpole from the surface of the object to the bottom of the banner and  $h_{min}$  is larger than or equal to 0.  $T$  is the thickness value at the current Profile Flag position. Another possibility to illustrate the thickness values is a spherical marker on the flagpole (see figure 4 (c)). The new concept of thickness visualization enables browsing of profiles with multiple Profile Flags without the need of inserting the cutting plane at the current location. Furthermore, one reference Profile Flag can be stuck at the position of a healthy profile. Areas with thickness differing from the reference profile can be easily located by browsing the underlying object with the help of a second Profile Flag.

### 3.2. Selection of Inspected Profiles

Up to now, the range selector has been an interface element which enables the selection of the visualized profiles. In our previous work [MEV\*05] just a conical range selector was used. The profiles of all surface positions covered by the base circle are simultaneously visualized on the banner. Extending the basic concept of the range selector enables also to indicate profiles with similar attributes. In the following we will call such a range selector a range indicator. We are not only interested in the spatial differences between profile locations, but also in the curve differences of the profiles themselves. Showing all the profiles around a Profile Flag where the profile difference is below a certain threshold generates

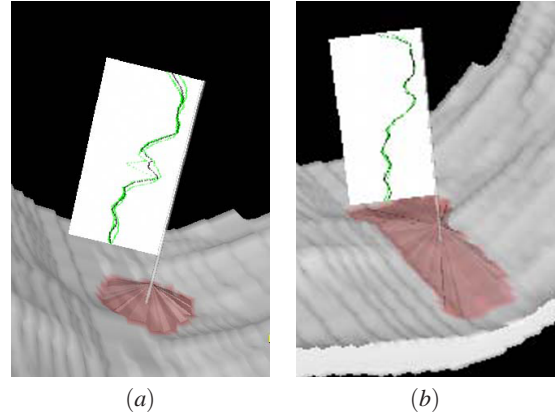


**Figure 6:** Profile Flag showing selection of profiles according to a certain criteria: (a) spatial-difference, (b) curve-difference.

range indicators with a polygonal base. This extension allows to illustrate the size and non-isotropic spread of a lesion. In this section, we discuss the spatial-difference as well as the curve-difference based specification of range indicators.

The selection of the set of profiles influences also the interaction with the cutting plane. For a Profile Flag showing a single profile, the cutting plane can be applied in order to show the  $T_2$  map in the neighborhood of the Flag. When selecting multiple profiles, the cutting plane can be moved forward and backward along the plane normal within the range of the selected profiles (see figure 5). This allows to inspect the entire set of selected profiles also in a slice-by-slice manner.

#### Spatial-difference range-indicator

In the basic concept, the range selector is positioned on the surface of the inspected surface. By changing the radius of the cone, all profiles located within the radius of the base circle are represented in the visualization. In addition to circular ranges now more general shapes, e.g., squares or arbitrary polygons are possible (see figure 6 (a)). An example would be to show on the banner the weighted average of all the profiles covered by the range indicator. This performs a convolution based noise removal. The kernel is given by the shape and size of the range indicator.

#### Curve-difference range-indicator

The range selector can be modified to enclose only those profiles, which fulfill certain criteria. Starting from the reference profile, located at the position of the needle, a set of neighboring profiles can be selected by region growing on the domain of profile curves. This guarantees that the result of the selection is a connected polygonal region whose profiles are "similar" to the reference profile.

The similarity criterion for profiles requires that a metric is defined on the profile curves. Let us assume that a profile curve  $P$  is given as a polyline consisting of  $n + 1$  points  $P_i$  with value  $V(P_i)$ . The difference between two profiles  $P, Q$  can be measured as the maximal point-wise difference  $\text{diff}(P, Q) = \max_{0 \leq i \leq n} |V(P_i) - V(Q_i)|$ . Another difference measure is the average point-wise difference:  $\text{diff}(P, Q) = \sum_{i=0}^n |V(P_i) - V(Q_i)| / n$ . Another way of specifying a set of profiles is threshold based:  $\{P \mid V(P_i) < T; \forall i \in (0, n)\}$ . Additionally one can subdivide the probed object along the needle into  $m + 1$  layers  $\{L_0, L_m\}$ . Then, defining a threshold for each layer, respectively, allows to detect profiles with suspicious characteristics with respect to their position along the needle (e.g., lesions near to the surface):  $\{P \mid V(P_i) < T_j; \forall i \in (0, n), j \in (0, m), P_i \in L_j\}$ .

A set of profiles is grown starting from the reference profile until the predefined threshold  $T$  or a difference threshold to the reference profile is exceeded. In general, using the range indicator, an arbitrary profile neighborhood can be defined by a combination of the spatial-difference and the curve-difference criteria. In order to compare two profiles with different lengths, one can apply the needle with adaptable length, which includes a fixed number of sampling positions irrespective of the profile length. Figure 6 (b) shows a Profile Flag representing a set of profiles with an average deviation smaller than a certain threshold.

### 3.3. Automatic Classification for Positioning of Profile Flags

An essential pre-processing step to the inspection of an object is the automatic positioning of the Profile Flags. In a medical environment we are usually interested in two types of profile data: a typical healthy profile and a suspicious profile significantly differing from the healthy one. With the help of Profile Flags, one or more suspicious profiles can be automatically depicted. Additionally, one Profile Flag can be used to depict a healthy profile as reference. The size of the suspicious area is visualized by an automatic selection of a set of profiles in the neighborhood of the detected profile. For the automatic positioning of the profiles, two types of classifications of the profiles can be used: model-based selection and statistics-based selection.

#### Model-based selection

With a model-based selection, we assume to have a shape model of the measured profiles. This model can be constructed either from an empirical study on a large set of healthy data or from a mathematical model of the profile. By evaluating all profiles within the dataset, one can find the healthy profile using the metrics discussed in the previous section.

#### Statistics-based selection

If just a small set of the inspected specimens is available or the specimens do strongly differ from each other, the model-based selection cannot be applied. In this case, a method can be based on a single specimen, assuming that the profiles in the healthy regions exhibit a similar shape. One can build a statistical model from a set of all available profiles within the data. By searching for a profile with the maximal or minimal deviation from the average model, the suspicious or healthy profiles can be defined. The advantage of this technique is that no model or database of healthy specimens is needed. A statistical-based selection mode is convenient for detecting relatively small features in the inspected data.

### 3.4. Probing of time-varying volume data

Our next modification of the original Profile Flag is concerned with time-varying 3D volumetric data. The profile information is then taken along the time axis. Previously, we probed the data along a line in 3D space, now we are profiling the temporal development at a specific 3D point location. When inspecting 3D time-varying data, where each spatial location corresponds to one profile, we need a different needle and range selector / range indicator (see figure 7). For measuring time-signal profiles, the needle tip is extended in the simplest case to a spherical range selector which encloses the selected profiles. The set of needles which extent into the temporal dimension is illustrated by black dots. The size of the selection sphere can be modified by moving a marker along the flag pole. In the more general case the range selector can be a general polytope including all time-signal profiles similar to the reference profile in the center. The shape of the range selector determines either the spatial size of the neighborhood or the value of the threshold used for the selection of the set of profiles. When visualizing temporal data, the horizontal axis usually corresponds to the time-axis. Therefore for time-varying data the banner visualizes the time-steps along the horizontal axis, while the vertical axis shows the values for each measured time-step. Additionally, for sparse temporal data (i.e., just a few time steps), vertical lines are included in order to facilitate reading off the values at particular time-steps.

## 4. Applications of Profile Flags

In this section we discuss two application areas of Profile Flags. In both cases the Profile Flag is guiding the inspecting radiologist to a suspicious profile by automatically positioning one or more Profile Flags. This reduces the time-consuming process of studying multiple volumetric sequences in a slice-by-slice manner. By dragging the Profile Flag, one can browse the profiles in the neighborhood of the detected profile. Another Profile Flag can be stuck into the investigated tissue in order to give a reference to a healthy profile. Finally the annotated tissue can be rendered as a sin-

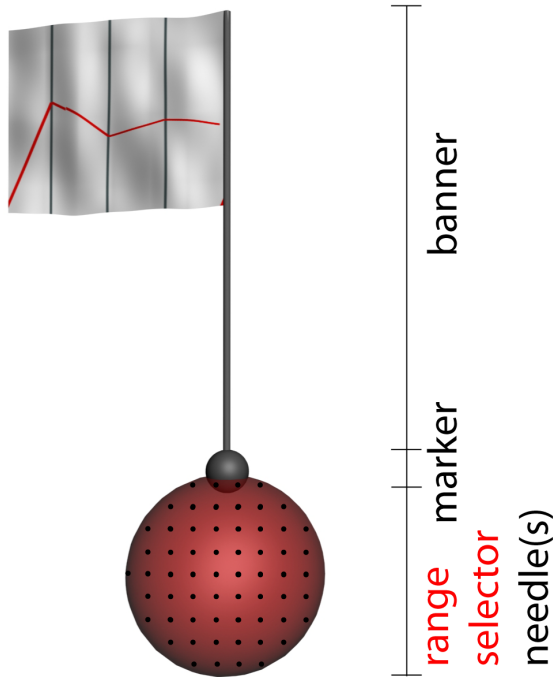


**Figure 7:** Extension of the Profile Flags for measurement of time-signal profiles.

gle image in contrast to rendering all slices with the suspicious profiles.

In section 4.1 we present an evaluation of inspecting knee-cartilage lesions. In section 4.2 we show the application of the Profile Flags for the detection of breast tumors.

#### 4.1. Inspection of knee-cartilage lesions

Twenty-nine semi-automatically pre-segmented specimens (7 healthy, 22 suspicious) have been investigated. The visualization of the data includes an automatic selection of suspicious profiles. The automatic selection of the most suspicious profile was performed by searching for the highest value in the  $T_2$  map within the cartilage. The size of the lesion is shown by region growing on the domain of profile curves. In this example we used the average point-wise difference to determine the shape of the lesion. The size of the lesion is denoted by the size and shape of the range indicator. Additionally, the average thickness of the cartilage in the selected region determines the height of the range indicator. Figure 8 shows a cartilage with a rather large lesion in the medial part. The cutting plane can be moved within the suspicious region in order to allow studying the  $T_2$  map in the selected area.

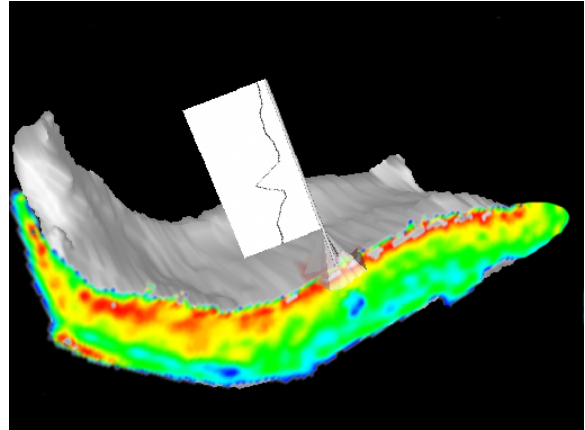


**Figure 8:** Cartilage lesion annotated by a Profile Flag.

#### Evaluation and discussion

In order to assess the value of the proposed visualization techniques, we have asked the medical partners from Catharina Hospital in Eindhoven to fill out a questionnaire. The questionnaire included over twenty figures with descriptions and open questions concerning the basic concept and the extensions of the Profile Flags. So far only two radiologists, who are experts on  $T_2$  maps, have filled in the questionnaire. It is clear that a larger study is necessary for statistically relevant conclusions. Here we give some qualitative findings that have emerged.

The evaluation has been performed by radiologists with good PC skills and above-average knowledge on medical workstations. At first glance, the concept of using Profile Flags seemed very interesting to the evaluators. Displaying the cutting plane with  $T_2$  maps at suspicious areas is helpful and essential for the diagnosis. Omitting the needle when showing the clipping plane is preferable as the  $T_2$  profile is not occluded at the needle position. The figures that did not contain the cutting plane with the  $T_2$  map were ranked lower in explanatory power than those showing the cross-section. The best rated technique among all presented methods was the visualization of the lesion shape through the range indicator. According to the radiologists, it helps to indicate the shape of the underlying lesion. However, this visualization is neither sufficient for the final diagnosis of the exact shape of the lesion nor for conveying the complete information about the  $T_2$  map. Insertion of the  $T_2$  map at the position of the needle adds the missing information. The respondents have chosen an image showing a Profile Flag with a selected set of profiles and a cutting plane as the most valuable and diagnostically-relevant visualization (similar to figure 5). This figure included a description of interaction with the cutting plane by moving it along its normal within the area of the range indicator. The next set of questions in the questionnaire dealt with the usability of rotating either the

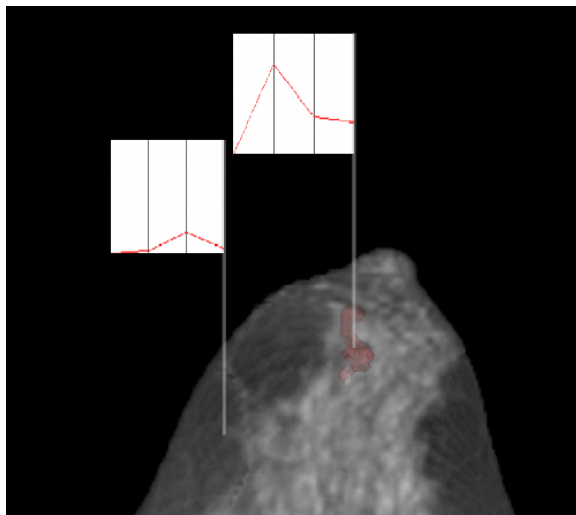


**Figure 9:** Two time-signal profiles annotated by Profile Flags: a healthy profile (left) and a malignant profile (right).

cutting plane or the object around the needle. No clear preferences were shown by the evaluators concerning the rotation of the cutting plane. This uncertainty might be due to low familiarity with object manipulations in 3D environments. The use of the deviation banner for showing the  $T_2$  profiles as a difference from a healthy profile has been rated as just a possible extension. This might be due to the fact that so far clinical inspections are based on absolute  $T_2$  values. The Profile Flags as a tool for annotation of damaged areas and for transferring the diagnosis to the orthopedists has been rated as very essential.

#### 4.2. Inspection of tumors in breast DCE-MRI data

Applying the previously described extensions, Profile Flags can be used for the exploration and the detection of tumors in breast DCE-MRI data. Figure 9 shows a visualization of the cancerous nodes in a patient's body. Two Profile Flags have been automatically positioned in the dataset: the left one is showing a healthy time-signal profile, while the right Profile Flag visualizes a set of suspicious profiles. The cost function for the automatic detection of the selected set of time-signal profiles is based on the model for tumor classification by Kuhl et al. [KMK\*99]. By dragging the Profile Flag over the 3D spatial domain, one can inspect the neighborhood of the automatically selected region.

#### 5. Summary and conclusions

In this paper we have presented two applications of probing dense but not homogenous data using Profile Flags. Several extensions of the basic Profile Flag concept, have been discussed. They are essential for the effective use of the glyph in

the context of specific application-oriented data. The extensions include selection of a set of profiles based on spatial as well as curve differences, automatic positioning of the Profile Flags, and adaptation for probing of time-varying volumetric data. The extensions have been tested on MR data in orthopedics and DCE-MRI data in mammography. Further, the preliminary evaluation of the techniques by our clinical partners have been described and discussed. With the extensions presented the Profile Flag is suitable for effective probing and sparse annotation of spatial and temporal profile data.

#### Acknowledgements

This work is funded by Philips Medical Systems in the scope of the COMRADE project (MRI based Visualization and Analysis for Virtual Colonoscopy and Orthopaedics). The DCE-MRI datasets used are courtesy of the MR Institut, Univ.-Klinik für Radiodiagnostik Innsbruck, Austria and the KH Lainz MRT Wien, Austria.

#### References

- [BG05] BRUCKNER S., GRÖLLER M. E.: VolumeShop: An interactive system for direct volume illustration. In *Proceedings of IEEE Visualization 2005* (2005), pp. 671–678.
- [CEP\*04] CAROTENUTO L., ERCOLANI M., PAS-SARIELLO R., CATALANO C., PEDICONI F., VENDITTI F.: Software tool for computer aided diagnosis of breast cancer in contrast enhanced MR sequences. In *EuroPACS-MIR 2004 in the Enlarged Europe* (2004), pp. 361–364.
- [CGB\*05] COTO E., GRIMM S., BRUCKNER S., GRÖLLER M. E., KANITSAR A., RODRIGUEZ O.: MammoExplorer: An advanced CAD application for breast DCE-MRI. In *Proceedings of Vision, Modelling, and Visualization 2005* (2005), pp. 91–98.
- [dLvW93] DE LEEUW W. C., VAN WIJK J. J.: A probe for local flow field visualization. In *Proceedings of IEEE Visualization 1993* (1993), pp. 39–45.
- [GAHS05] GOETZELMANN T., ALI K., HARTMANN K., STROTHOTTE T.: Adaptive labeling for illustrations. In *Proceedings of Pacific Graphics 2005* (2005), pp. 64–66.
- [HvL00] HUITEMA H., VAN LIERE R.: Interactive visualization of protein dynamics. In *Proceedings of IEEE Visualization 2000* (2000), pp. 465–468.
- [KMK\*99] KUHL C. K., MIELCARECK P., KLASCHIK S., LEUTNER C., WARDELMANN E., GIESEKE J., SCHILD H. H.: Dynamic breast MR imaging: Are signal intensity time data useful for differential diagnosis of enhancing lesions? *Radiology* 211, 1 (1999), 101–110.
- [KPWP02] KOHLE S., PREIM B., WIENER J., PEITGEN



- H.-O.: Exploration of time-varying data for medical diagnosis. In *Proceedings of Vision, Modelling, and Visualization 2002* (2002), pp. 131–138.
- [MEV\*05] MLEJNEK M., ERMES P., VILANOVA A., VAN DER RIJST R., VAN DEN BOSCH H., GERRITSEN F., GRÖLLER M. E.: Profile flags: a novel metaphor for probing of  $T_2$  maps. In *Proceedings of IEEE Visualization'05* (2005), pp. 599–606.
- [MTB03] MCGUFFIN M. J., TANCAU L., BALAKRISHNAN R.: Using deformations for browsing volumetric data. In *Proceedings of IEEE Visualization 2003* (2003), pp. 401–408.
- [PTSP02] PREIM B., TIETJEN C., SPINDLER W., PEITGEN H. O.: Integration of measurement tools in medical 3D visualizations. In *Proceedings of IEEE Visualization 2002* (2002), pp. 21–28.
- [RGWW05] RECHT M. P., GOODWIN D. W., WINALSKI C. S., WHITE L. M.: MRI of articular cartilage: Revisiting current status and future directions. *American Journal of Roentgenology* 184, 4 (2005), 899–914.
- [SBC04] SUBRAMANIAN K., BROCKWAY J., CARRUTHERS W.: Interactive detection and visualization of breast lesions from dynamic contrast enhanced MRI volumes. *Computerized Medical Imaging and Graphics* 28, 8 (2004), 435–444.
- [SMD\*01] SMITH H. E., MOSHER T. J., DARDZINSKI B. J., COLLINS B. G., COLLINS C. M., YANG Q. X., SCHMITHORST V. J., SMITH M. B.: Spatial variation in cartilage T2 of the knee. *J Magn Reson Imaging* 14 (2001), 50–55.
- [vdRvdBK\*03] VAN DER RIJST R. H., VAN DEN BOSCH H., KNOWLES A., KORTMAN J. H., WONDERGEM J. H.: High resolution quantitative imaging of patellar cartilage defects at 1.5T. *Proc. Intl. Soc. Mag. Reson. Med.* 11 (2003), 442.
- [VKG05] VIOLA I., KANITSAR A., GRÖLLER M. E.: Importance-driven feature enhancement in volume visualization. *IEEE Transactions on Visualization and Computer Graphics* 11, 4 (2005), 408–418.